ARTICLE
Journal of Cellular Biochemistry 112:1093–1102 (2011)

Journal of Cellular Biochemistry

Electrophysiological Characterization of Potassium Conductive Pathways in *Trypanosoma cruzi*

Veronica Jimenez,[1,2]* Mauricio Henriquez,[3] Norbel Galanti,[1] and Gloria Riquelme[3]

[1]*Programa de Biologia Celular y Molecular, Instituto de Ciencias Biomedicas, Facultad de Medicina, Universidad de Chile, Santiago, Chile*

[2]*Center for Tropical and Emerging Global Diseases, University of Georgia, Athens, Georgia*

[3]*Programa de Fisiologia y Biofisica, Instituto de Ciencias Biomedicas, Facultad de Medicina, Universidad de Chile, Santiago, Chile*

ABSTRACT

Potassium channels (K^+ channels) are members of one of the largest and most diverse families of membrane proteins, widely described from bacteria to humans. Their functions include voltage-membrane potential maintenance, pH and cell volume regulation, excitability, organogenesis and cell death. K^+ channels are involved in sensing and responsing to environmental changes such as acidification, O_2 pressure, osmolarity, and ionic concentration. *Trypanosoma cruzi* is a parasitic protozoan, causative agent of Chagas disease (American trypanosomiasis) an endemic pathology in Latin America, where up 200,000 new cases are reported annually. In protozoan parasites, the presence of K^+ channels has been suggested, but functional direct evidence supporting this hypothesis is limited, mainly due to the difficulty of employing conventional electrophysiological methods to intact parasites. In *T. cruzi*, K^+ conductive pathways are thought to contribute in the regulatory volume decrease observed under hyposmotic stress, the steady state pH and the compensatory response to extracellular acidification and the maintenance of plasma membrane potential. In this work we describe the isolation of plasma membrane enriched fractions from *T. cruzi* epimastigotes, their reconstitution into giant liposomes and the first functional characterization by patch-clamp of K^+ conductive pathways in protozoan parasites. J. Cell. Biochem. 112: 1093–1102, 2011.

KEY WORDS: CHANNELS; ELECTROPHYSIOLOGY; MEMBRANE; TRYPANOSOMA

Potassium channels (K^+ channels) belong to one of the largest and most diverse family of membrane proteins, widely described from bacteria to man [Derst and Karschin, 1998; MacKinnon et al., 1998; Morais Cabral et al., 1998; Zhou and MacKinnon, 2004; Long et al., 2005, 2007]. They are involved in membrane potential maintenance, pH and cell volume regulation, excitability, organogenesis and cell death and many other cellular processes [Bae et al., 1999; Hille, 2001; Lang et al., 2005; Park et al., 2007]. In different cell types, sensing and responsing to environmental changes such as acidification, O_2 pressure, osmolarity and ionic concentration are dependent on K^+ channel activity [Lahiri et al., 2006; Kemp and Peers, 2007; Almanza et al., 2008; Hughes and Swaminathan, 2008]. In protozoan parasites, the presence of this type of conductive pathway has been suggested [Vieira and Cabantchik, 1995; Ponte-Sucre et al., 1998, 2001; Nolan and Voorheis, 2000; Van der and Docampo, 2000, 2002; Rohloff et al., 2003] but functional direct evidence supporting this hypothesis is scant, mainly because of the difficulty in using conventional electrophysiology on intact parasites.

Recently, two putative K^+ channels (PfK1 and PfK2) from *Plasmodium falciparum*, an important human protozoan pathogen, have been cloned and characterized at the molecular level [Ellekvist et al., 2004; Waller et al., 2008b]. Furthermore, sexual reproduction of the mosquito-stage of *Plasmodium bergei* seems to be impaired by gene disruption of *pbKch1*, the homologous gene for *pfKch1* (PfK1) in this parasite [Ellekvist et al., 2008], suggesting that K^+ channels could be a potential therapeutic targets against parasitic diseases [Ellekvist and Colding, 2006; Waller et al., 2008a].

N. Galanti and G. Riquelme contributed equally to this work.

Grant sponsor: American Heart Association-USA; Grant number: 09POST2200011; Grant sponsor: FONDECYT-Chile; Grant number: 1090124; Grant sponsor: Proyecto Bicentenario Anillo de Investigación en Ciencias y en Tecnología-Chile; Grant number: ACT112; Grant sponsor: FONDECYT-Chile; Grant number: 1070695.

*Correspondence to: V. Jimenez, Center for Tropical and Emerging Global Diseases, University of Georgia, 500 DW Brooks Dr, Paul Coverdell Center Room 350, Athens, GA 30602. E-mail: vjimen@uga.edu

Received 3 January 2011; Accepted 5 January 2011 • DOI 10.1002/jcb.23023 • © 2011 Wiley-Liss, Inc.
Published online 18 January 2011 in Wiley Online Library (wileyonlinelibrary.com).

In *Trypanosoma cruzi*, the causative agent of Chagas disease, K^+ conductive pathways have been postulated to play a role in osmoregulatory process, contributing to 7% of the regulatory volume decrease observed under hyposmotic stress [reviewed in Rohloff and Docampo, 2008]. On the other hand, pH steady state and the compensatory response to extracellular acidification are K^+ dependent in *T. cruzi* mammalian stages, both process being Ba^{+2} and Cs^+ sensitive [Van der and Docampo, 2000]. These authors pointed to an inward rectifier K^+ channel as one of the effectors participating in parasite pH homeostasis.

In most cells, plasma membrane potential (Vm) is maintained through Na^+/K^+ ATPases operating together with K^+ channels, generating the necessary ion gradients that drive multiple transport mechanisms. *T. cruzi* Vm is mainly dependent on a H^+-ATPase but in trypomastigotes (mammalian stage), Vm variations are highly sensitive to extracellular K^+ concentrations, suggesting that passive K^+ conductive pathways are present in the plasma membrane [Van der and Docampo, 2002].

Characterization and functional conclusive demonstration of channel activity requires direct electrophysiological methods. In this regard, the most powerful tool is the patch-clamp technique, which allows for single-channel recording [Hamill et al., 1981]. Unfortunately, the small size and active motility of *T. cruzi* makes this approach extremely difficult. To overcome this limitation, we isolated membranes from epimastigotes (triatomine bug stage) that were subsequently reconstituted into giant liposomes [Riquelme et al., 1990] and recorded by patch-clamp, to obtain the first functional characterization of K^+ conductive pathways in *T. cruzi*.

MATERIALS AND METHODS

PARASITES CULTURE

T. cruzi epimastigotes (Tulahuen strain) were grown at 28°C in Diamond's liquid medium (106 mM NaCl, 29 mM KH_2PO_4, 23 mM K_2HPO_4, 12.5 g/L tryptose, 12.5 g/L tryptone, and 12.5 g/L yeast extract, pH 7.2) supplemented with 10% fetal bovine serum, 7.5 μM hemin, and antibiotics (penicillin 75 U/ml-streptomycin 75 μg/ml) [Diamond, 1968].

MEMBRANE ISOLATION

Purification of *T. cruzi* epimastigote membranes was achieved using previously described methods [Benaim et al., 1991]. Briefly, parasites at the exponential phase of growth were collected by centrifugation at 1,000*g* for 10 min and washed twice with five volumes of washing buffer (10 mM KCl, 140 mM NaCl, 75 mM Tris–Cl pH 7.4). The pellet was resuspended in lysis buffer containing 400 mM mannitol, 10 mM KCl, 2 mM EDTA, 1 mM PMSF, 10 μg/ml leupeptin, 5 μg/ml aprotinin, 20 mM HEPES-K pH 7.4. The controlled lysis of the parasites was done by freeze-thaw three times in liquid nitrogen followed by glass-teflon homogenization.

After differential centrifugation at 1,000*g* for nuclei separation, and at 16,000*g* for 30 min to eliminate mitochondria, a microsomal fraction enriched in plasma membrane was obtained by centrifugation of the supernatant at 100,000*g* 1 h. The final pellet was resuspended in 150 mM NaCl, 10 mM HEPES-K pH 6.8 containing protease inhibitors mix and stored in liquid nitrogen. Integrity of membrane vesicles and cross-contamination with other organelles were evaluated by electron microscopy.

RECONSTITUTION OF ISOLATED MEMBRANES INTO GIANT LIPOSOMES

Giant liposomes were prepared according to the method reported by Riquelme et al. [1990]. A membrane aliquot containing 50–100 μg of protein was mixed with 2 ml of a 13 mM (in terms of lipid phosphorus) suspension of the asolectin vesicles. After a partial dehydration/rehydration cycle, the diameter of the resulting giant multilamellar liposomes ranged from 5 to 100 μm.

PATCH-CLAMP RECORDINGS

Aliquots (3–5 μl) of giant liposomes were placed into the recording chamber (RC-28, Warner Instruments Corporation, USA) mixed with 0.4 ml of the buffer of choice for electrical recording (bath solution). Single-channel recordings were obtained by patch-clamp [Hamill et al., 1981]. Giga seals were formed on giant liposomes with glass-microelectrodes of 5–10 MΩ resistance. After sealing, withdrawal of the pipette from the liposome surface resulted in an excised patch. Current was recorded with an EPC-9 amplifier (Heka Elektronic, Lambrecht/Pfalzt, Germany) at a gain of 50–100 mV/pA and a filter setting of 10 kHz. The holding potential was applied to the interior of the patch pipette, and the bath was maintained at virtual ground ($V = Vbath - Vpipette$). The bath was grounded via an agar bridge and the junction potential was compensated when necessary. The signal was analyzed off-line using TAC (Bruxton Corporation), Pulse Fit (Heka, Lambrecht/Pfalz) and Microcal Origin 7.0 (Microcal Software, Inc., USA) software. All the experiments were conducted at room temperature.

SOLUTIONS

Pipette and bath solutions had the following composition: 140 mM KCl, 10 mM HEPES-K pH 7.4. Cationic selectivity was analyzed replacing KCl in bath solution for 140 mM K gluconate or 140 mM NMDG-Cl (N-methyl-D-glucamine chloride). For the monovalent cation selectivity experiments, K^+ was replaced by Na^+, Cs^+, Li^+, or NH_4^+. Divalent cation permeability was tested replacing the bath solution for the following buffers (in mM):

20 $CaCl_2$, 40 KGluconate, 100 KCl; 10 HEPES-K pH 7.4.
20 $MgCl_2$, 40 KGluconate, 100 KCl; 10 HEPES-K pH 7.4.
20 $BaCl_2$, 40 KGluconate, 100 KCl; 10 HEPES-K pH 7.4.

To evaluate the blocking effect of calcium, BAPTA-K_4 was used as chelator and calcium-free concentration (from 0 to 1 mM) was calculated according to MaxChelator software (C. Patton, University of Stanford, USA).

Bath solution was replaced by the following buffers (in mM):

- Calcium free: 134 KCl, 2 BAPTA-K_4, 10 HEPES-K pH 7.4.
- pCa 5: 132 KCl, 2 BAPTA-K_4, 1.68 $CaCl_2$, 10 HEPES-K pH 7.4.
- pCa 4: 132 KCl, 2 BAPTA-K_4, 2.1 $CaCl_2$, 10 HEPES-K pH 7.4.
- pCa 3: 132 KCl, 2 BAPTA-K_4, 3 $CaCl_2$, 10 HEPES-K pH 7.4.

pCa is defined as $-\log [Ca^{+2}]$ where $[Ca^{+2}]$ refers to free calcium concentration in a 0.15 M ionic strength solution, at 20°C.

Magnesium blocking effect was tested replacing the bath solution for the following buffers (in mM):

- 1 $MgCl_2$, 138 KCl, 10 HEPES-K pH 7.4.
- 5 $MgCl_2$, 130 KCl, 10 HEPES-K pH 7.4.
- 20 $MgCl_2$, 100 KCl, 10 HEPES-K pH 7.4.

DATA ANALYSIS

Data were expressed as means ± standard error of the mean (SEM). Statistical differences were tested by two populations Student *t*-test or ANOVA. Normal distribution and homogeneity of variance were analyzed by the Levene test.

RESULTS

ELECTROPHYSIOLOGICAL RECORDINGS IN ISOLATED MEMBRANES FROM *T. CRUZI* EPIMASTIGOTES

Technical limitations to gain access to intact *T. cruzi* parasites for patch-clamp recordings are related with motility, size and shape of the parasites, as well as the presence of a strong microtubular network localized underneath the plasma membrane [Gull, 1999]. A good alternative methodology is the reconstitution of ion channels into artificial lipid membranes. A microsomal fraction enriched in plasma membrane was isolated by differential centrifugation from *T. cruzi* epimastigotes at the exponential phase of growth (Fig. 1).

This isolation method was developed based on previous work, demonstrating that cell disruption under hypertonic conditions followed by differential centrifugation, allows the isolation of

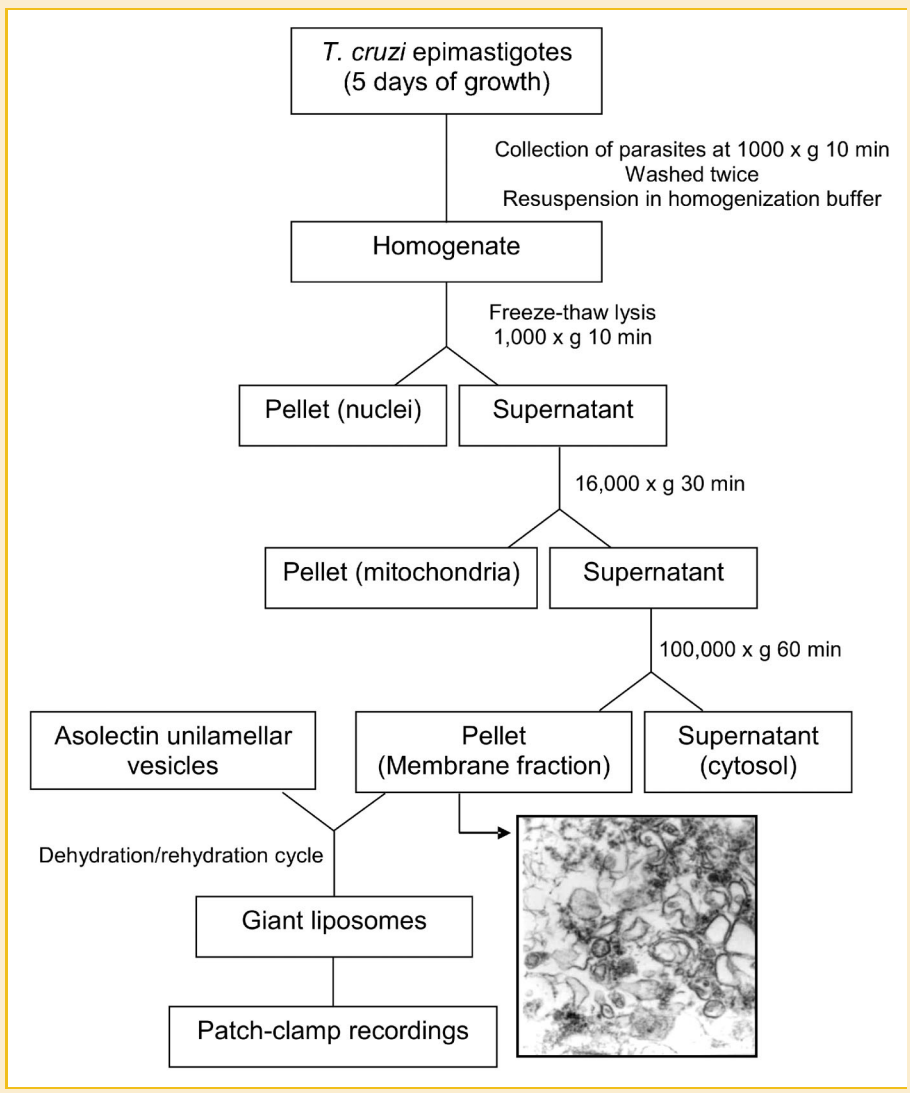

Fig. 1. *T. cruzi* epimastigote membranes isolation and reconstitution into giant liposomes. Tulahuen strain epimastigote fractionation was performed as indicated in the Materials and Methods Section. Isolated membranes were reconstituted into giant liposomes and channel activity was recorded by patch-clamp. Insert: Transmission electron microscopy of membrane fraction obtained following the protocol presented above. Magnification: 69,000×.

plasma membrane vesicles from *T. cruzi*. These vesicles are tightly closed and suitable for determination of ion transport [Benaim et al., 1995; Martinez et al., 2002]. Cross contamination with other organelles was evaluated by transmission electron microscopy (Fig. 1) and considered negligible for the following procedure of giant liposome/plasma membrane preparation.

Plasma membrane enriched fractions obtained from 10 independent axenic cultures, were reconstituted into asolectin giant liposomes [Riquelme et al., 1990]. Giga seals with appropriate signal-noise ratio were obtained by patch-clamp method in 146 (76%) of 196 patches showing stable electrical activity. These results indicate that the reconstitution method is reliable and highly efficient in terms of electrical activity to characterize single channel currents.

POTASSIUM CONDUCTIVE PATHWAYS IN *T. CRUZI* EPIMASTIGOTES

In 11 of 63 patches analyzed (17%), a potassium conductive pathway was detected under identical KCl concentration in the bath and the pipette (symmetrical conditions). In fact, when an increasing positive voltage step pulse protocol was applied, a single current level was observed with higher open probability in comparison with negative pulses (Fig. 2A, +80 mV step). When the bath solution was replaced to establish asymmetrical potassium conditions (140 and 40 mM K^+ pipette and bath, respectively) the reversal potential shifted from 0 (Fig. 2B, gray line) to 18.8 ± 3.7 mV ($n = 5$) when a voltage ramp from −120 to +120 mV was applied (Fig. 2B, black line), indicating a potassium conductivity (theoretical equilibrium potential for potassium +32 mV).

The calculated relative permeability ratio P_K/P_{Cl} was 5.03 ± 0.7 ($n = 5$) showing that selectivity for potassium respect to chloride is not extremely high for this channel.

A linear single channel current–potential relationship and a reversal potential of 0 mV was observed under symmetrical condition (KCl 140 mM in bath and pipette) (Fig. 2C). Under these conditions, the single-channel conductance calculated as the I/V slope was 106 ± 4.3 pS ($n = 4$).

The low frequency of these type of currents in plasma membranes of *T. cruzi* epimastigotes impaired further characterization regarding ion selectivity and blockage sensitivity.

ELECTROPHYSIOLOGICAL CHARACTERIZATION OF A NON-SELECTIVE CATION CHANNEL

The most frequent activity recorded in *T. cruzi* epimastigote plasma membrane vesicles reconstituted in liposomes corresponds to a Non-Selective Cation Channel (TcNSCC). Applying a voltage step pulse, a characteristic current was observed being more active at positive potentials (Fig. 3A). The channel activity was frequently observed in clusters as it is shown in Figure 3B, where at least four levels of current can be detected. Each level corresponds to the unitary current belonging to a single channel. The chord conductance calculated at +80 mV and −80 mV was 65.1 ± 4 pS and 45.4 ± 2 pS respectively ($n = 12$) indicating a non-linear current–voltage relationship (Fig. 3C).

When a voltage ramp from +120 to −120 mV was applied under KCl symmetrical conditions (140 mM KCl in bath and pipette), the reverse potential was near to 0 mV (Fig. 4A black line). A shift to

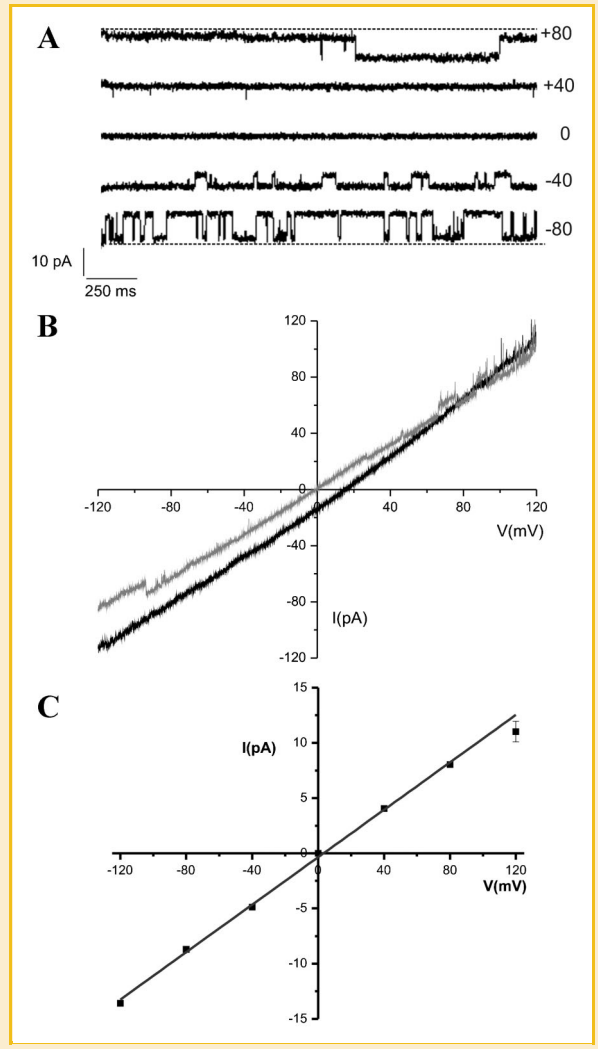

Fig. 2. Potassium currents from *T. cruzi* epimastigotes. A: Representative current traces applying a voltage-step protocol at the indicated potentials. The recording was obtained under symmetrical conditions with bath and pipette solution containing 140 mM KCl, Hepes K 10 mM pH 7.4. Dash lines indicate open state. B: Current traces obtained with a voltage-ramp protocol. Under symmetrical conditions (gray line) with bath and pipette solutions indicated in (A) the reverse potential was near to 0 mV. Replacing the bath solution for 40 mM KCl, Hepes K 10 mM pH 7.4 (black line) a shift in the reverse potential to +18.8 mV was observed. C: Current–voltage relationship under symmetrical conditions described in (A). Data correspond to the unitary current obtained at the indicated potentials in a continuous pulse protocol. Conductance calculated from the slope was 106 ± 4.3 pS ($n = 4$). Black line corresponds to the best fit of the data to a linear equation.

-20 ± 3 mV ($n = 8$) was observed in the reverse potential when the bath solution was replaced by 300 mM KCl (Fig. 4A gray line), near to the calculated theoretical reverse potential for K^+ under these conditions (−19.6 mV). Based on the experimental reverse potentials measured under asymmetrical conditions, the relative permeability ratio between K^+ and Cl^- was calculated. The P_K/P_{Cl} obtained was 19.2 ± 1.1 ($n = 6$), suggesting that this channels has a strong selectivity for cations over anions.

In order to confirm the cationic selectivity of TcNSCC, a current–voltage relationship was calculated from a voltage step pulse

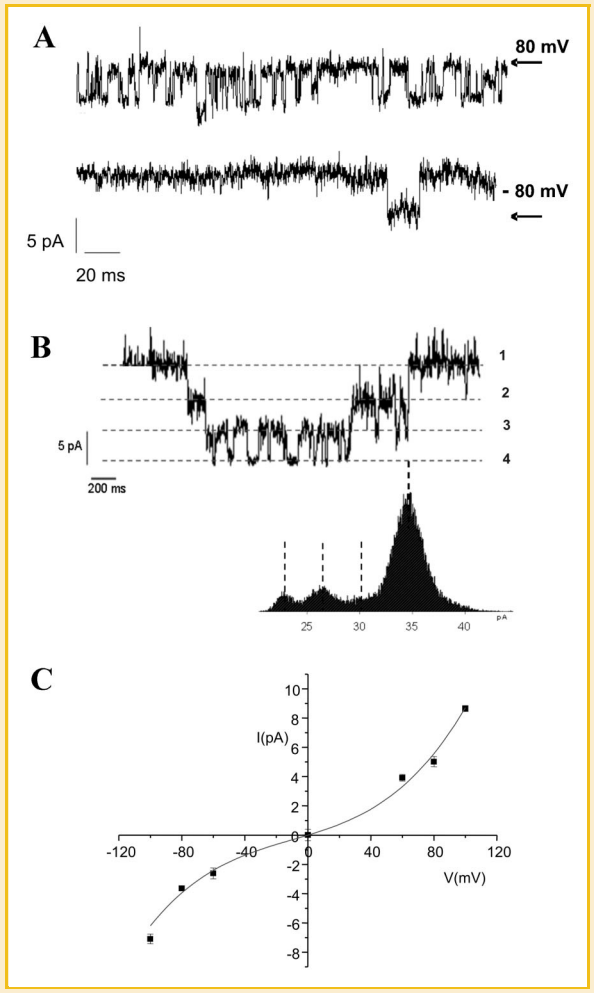

Fig. 3. General characteristics of TcNSCC currents. A: Representative current traces at the indicated potentials under symmetrical conditions with bath and pipette solution containing 140 mM KCl, Hepes K 10 mM pH 7.4. Arrows indicate the open state of the channel. B: Recording at +80 mV where multiple level of current were observed (dot lines) in the same patch. Histogram represents the frequency of each current level, which corresponds to multiple of the unitary current (~5 pA). C: Current–voltage relationship under symmetrical conditions described in (A). Data correspond to the unitary currents recorded in continuous voltage steps. The calculated unitary conductance was near to 65 pS at +80 mV and 45 pS at −80 mV indicating a slight rectification of the current in both directions. Black line is the best fit to the data according to Boltzman equation.

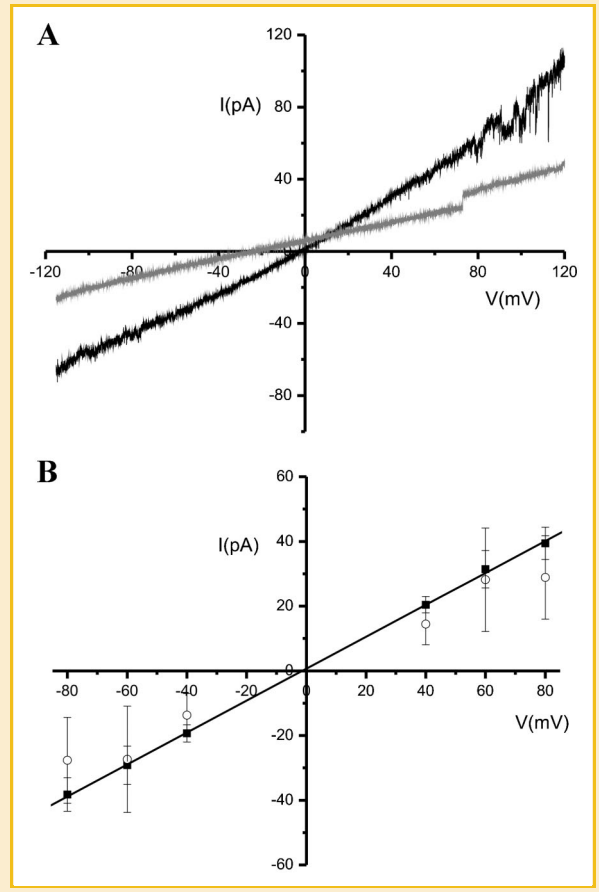

Fig. 4. Monovalent cation selectivity of TcNSCC. A: Current traces applying a voltage-ramp protocol under symmetrical (black line) or asymmetrical (gray line) conditions. B: Relationship between the potential and the total current of the seal, obtained from a voltage-step protocol under symmetrical condition described in (A) (black squares) or replacing the bath solution for 140 mM K-gluconate, Hepes-K 10 mM pH 7.4 (open circles).

protocol, applied under symmetrical conditions (Fig. 4B, black squares) or replacing the bath solution by 140 mM potassium gluconate (Fig. 4B, open circles). As expected, no significant change in the current amplitude or shift in the reverse potential was observed, confirming the low anion conductance of TcNSCC.

When K^+ was replaced by Na^+ in the bath solution, the reverse potential shifted to +8.8 mV (Table I), obtaining a calculated relative permeability ratio Na^+/K^+ of 0.72, as is expected for a non-selective cation channel. Selectivity for other monovalent cations was analyzed by replacing K^+ with Cs^+, Li^+, or NH_4^+ in the bath solution and applying a voltage ramp from +120 to −120 mV. Relative permeability ratios for each cation were calculated according to the derived equation from Goldman–Hodgkin–Katz:

$$P_X/P_K = ([K]_i \exp(FV/RT) - [K]_o / \exp(FV/RT)[X]_i$$

where P_X is the cation X permeability, P_K is the potassium permeability, F is the Faraday constant, R is the gas constant, T is the absolute temperature, V is the experimental change in the reverse potential, $[K]_i$ correspond to potassium concentration in the bath, $[K]_o$ is the potassium concentration in the pipette and $[X]_i$ represents the monovalent cation concentration in the bath.

The permeability sequence obtained was: $NH_4^+ \cong Cs^+ > K^+ > Na^+ > Li^+$ with values of 1.16, 1.15, 1.0, 0.72, and 0.55. NMDG permeability was 0.11 as expected for a non-permeable cation (Table I).

TcNSCC permeability to divalent cations was assessed maintaining symmetrical concentrations for KCl and adding 20 mM $CaCl_2$ to the bath solution. In response to a voltage ramp from 120 mV to −120 mV the reverse potential observed was −0.72 mV (data not shown), suggesting low calcium permeability or a possible blockage by this cation. Relative permeability ratio for Ca^{+2}, Mg^{+2}, and Ba^{+2} was calculated following the derived Goldman–Hodgkin–

TABLE I. TcNSCC Selectivity for Monovalent Cations

X	ΔV_{rev} (mV)	P_X/P_K	N
K	0.0	1.0	–
Na	+8.8 ± 2.4	0.72 ± 0.05	2
Cs	−3.3 ± 0.2	1.15 ± 0.003	2
Li	+13.9 ± 0.7	0.55 ± 0.04	2
NH_4	−3.5 ± 0.3	1.16 ± 0.01	2
NMDG	+45.8 ± 6.5	0.11 ± 0.09	8

Relative permeability ratios for monovalent cations respect to potassium were calculated according to Goldman–Hodgkin–Katz equation with the experimental reverse potential obtained under bi-ionic condition. Data are expressed as means ± SEM. N correspond to number of independent experiments analyzed.

Katz equation at the steady state where the current is zero:

$$I = P_K z_K F \xi \frac{[K]_i - [K]_o e^{-\xi}}{1 - e^{-\xi}} + P_D z_D F \xi \frac{[D]_i - [D]_o e^{-\xi}}{1 - e^{-\xi}} = 0$$

where I is the current through the patch, P_K is the permeability of potassium, z_K is the valence of potassium, F is the Faraday constant, ξ is the FV/RT where V is the shift in the experimental reverse potential, $[K]_i$ and $[K]_o$ correspond to potassium concentration in the bath and pipette respectively, P_D is the permeability for the divalent cation, z_D is the valence of the divalent cation, $[D]_i$ and $[D]_o$ are the divalent cation concentrations in the bath and pipette respectively. Considering the experimental conditions the derived equation is:

$$\frac{P_D}{P_K} = \frac{[K](1 - e^{2\varepsilon})}{4[D]_i e^{2\varepsilon}}$$

The calculated relative permeability ratio for Ca^{+2} and Mg^{+2} was 0.10 and 0.09 respectively, suggesting a low permeability for both divalent cations (Table II). In accordance with these values, the shift in the reverse potential was negligible. When 20 mM $BaCl_2$ was added to the bath solution, the reverse potential shifted to −5.7 mV ± 1.3 (Table II). The calculated permeability ratio P_{Ba}/P_K based on the experimental reverse potential was close to 1. Under symmetrical conditions for K^+, the presence of 20 mM Ba^{+2} slightly decreased the currents recorded when a voltage step protocol was applied, suggesting a possible blocking effect of the divalent ion (data not shown).

Because divalent cations have been previously described as blockers of non-selective cation channels [Llanos et al., 2002], the effect of calcium on TcNSCC currents was investigated. Replacing the bath solution by buffers with controlled free calcium concentrations (see Materials and Methods Section) a decrease in the patch total current was observed. The percentage of current reduction was dependent on the calcium concentration. Consequently a linear dose-dependent response was observed when different voltage step pulses were applied, even in the presence of 10 μM calcium. The effect was reverted when the bath solution was replaced by calcium-free buffer (Fig. 5A).

TABLE II. TcNSCC Selectivity for Divalent Cations

X	ΔV_{rev} (mV)	P_D/P_K	N
K	0.0	1.0	–
Ca	−0.73 ± 0.3	0.10	4
Mg	−0.59 ± 0.4	0.09	3
Ba	−5.72 ± 1.3	1.05	3

Relative permeability ratios for divalent cations respect to potassium were calculated according to Goldman–Hodgkin–Katz equation derivate for symmetrical potassium conditions in the presence of 20 mM divalent cations. Chloride was maintained symmetric adjusting the anion concentration with gluconate. Data are expressed as means ± SEM.

The Ki (inhibition constant) was calculated according to the binding equation [Sabirov et al., 2001]:

$$i = i_o/(1 + A/Ki)$$

where *i* is the total current in the patch without calcium, i_o is the current after calcium addition and A is the divalent cation concentration. The values obtained were 0.54 ± 0.043 mM (Fig. 5B, black circles) and 0.50 ± 0.042 mM (Fig. 5B, open circles) for positive and negative potentials, respectively.

The blocking effect was partial, with a residual current in the presence of 20 mM calcium that reaches 20% of the maximum current recorded in the absence of divalent cation (data not shown). This effect can be explained by an incomplete blockage or by different types of channels present in the same seal, with only some being calcium-sensitive.

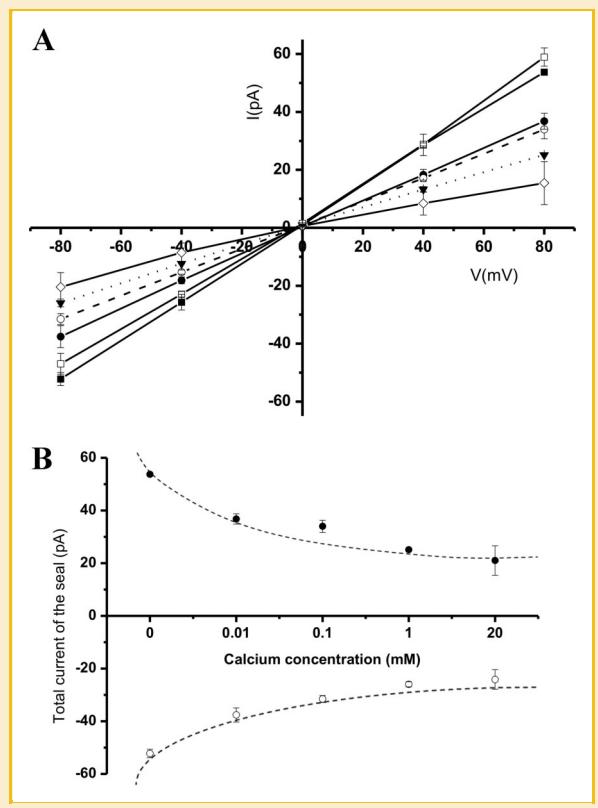

Fig. 5. Blockage of TcNSCC by calcium. A: Voltage–current relationship obtained from total currents of the seal recorded applying a voltage-step protocol from −80 to +80 mV under symmetrical condition for potassium and controlled calcium concentrations (calcium was adjusted according to the calculated pCa). Control: black squares, 10 μM black circles, 100 μM open circles, 1 mM black triangles, 20 mM open diamonds, wash open squares. B: Total current of the seal recorded at −80 (open circles) and +80 mV (black circles), under symmetrical condition described in (A) and increasing calcium concentration. Kd_s were calculated according to the binding equation. Lines correspond to the best fit of the data to the equation.

Additionally, we tested the effect of magnesium over TcNSCC activity. In the presence of 20 mM $MgCl_2$ in the bath solution, a reversible reduction of the patch total current was also observed (Fig. 6A). The percentage of the total current of the patch (in the presence of Mg^{+2} relative to the current in the absence of the divalent ion) corresponds to $43.2 \pm 6\%$ at +80 mV and $61.5 \pm 6\%$ at −80 mV. Recordings of the single channel current when a voltage pulse of −80 mV was applied in the presence of 5 mM $MgCl_2$, showed reduction in the unitary current from −4.8 to −1.8 pA (data not shown). The estimated Ki_s for Mg^{+2} were similar for positive and negative potentials, with values of 11.7 ± 2.9 mM (Fig. 6B, black circles) and 10.5 ± 2.7 mM respectively (Fig. 6B, open circles). Similar to other non-selective cation channels previously described, TcNSCC was insensitive to amiloride or lanthanum and slightly sensitive to 100 μM flufenamic acid (data not shown).

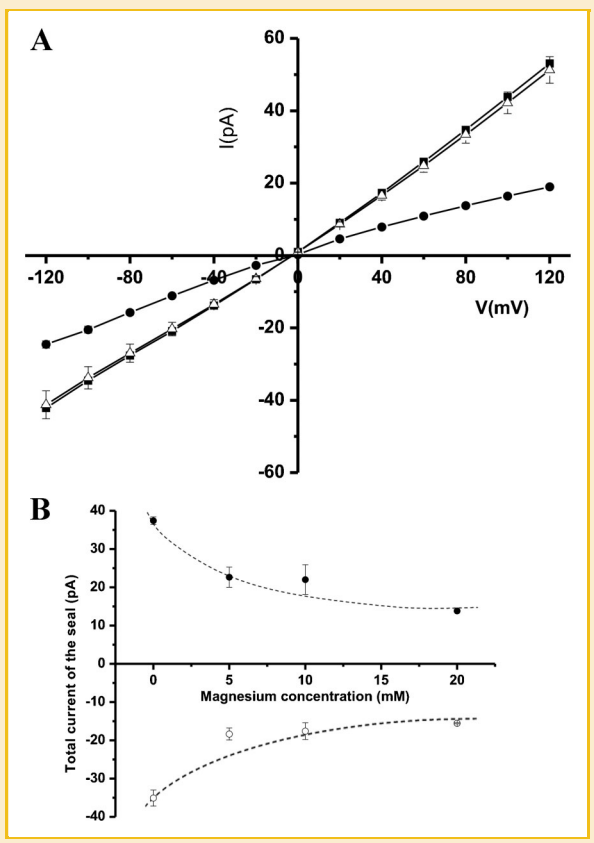

Fig. 6. Magnesium effect on TcNSCC. A: Voltage–current relationship obtained from total currents of the seal recorded applying a voltage-step protocol from −120 to +120 mV under symmetrical condition for potassium (bath and pipette solutions 140 mM KCl, Hepes K 10 mM pH 7.4. black squares) or in the presence of 20 mM $MgCl_2$ (black circles). The effect was completely reverted by washing with 140 mM KCl, 10 mM Hepes K pH 7.4 (open triangles). B: Total current of the seal recorded at −80 (open circles) and +80 mV (black circles), under symmetrical condition described in (A) and increasing magnesium concentration. Kd_s were calculated according to the binding equation. Lines correspond to the best fit of the data to the equation.

DISCUSSION

The data presented in this work constitute the first electrophysiological demonstration of *T. cruzi* ion channel activity. Direct measurement of parasite membranes by conventional recording methods has been limited by intrinsic characteristics of the cells. The active motility introduces a level of noise and instability on the seals non acceptable for single-channel studies. Furthermore, the small size, a non-regular shape and a complex subpellicular cytoskeleton [Gull, 1999] make very difficult the excised patch or the cell-attached configurations on intact cells.

The isolation of cell membranes and further reconstitution into an artificial lipidic matrix, has been extensively used as an alternative methodology for the characterization of ion channels from diverse cell types [Berrier et al., 1989; Hosokawa et al., 1994; Bai and Shi, 2001; Henriquez and Riquelme, 2003; Wyneken et al., 2004; Barrera et al., 2005; Bernucci et al., 2006], validating the data obtained through this methodology with the ones recorded under more physiological conditions. Although in this report *T. cruzi* membrane orientation on the giant liposomes was not investigated, previous studies performed with ligand-activated channels demonstrated that the insertion occurs mainly in the right direction, which means with the extracellular side of the protein facing outside [Riquelme et al., 1990].

The method of isolation of a plasma membrane enriched fraction has previously proven to be adequate for obtaining closed vesicles with minimum leakage, negligible contamination with mitochondria or other organelles and no microtubules attached to the membranes [Nagakura et al., 1986; Benaim et al., 1991, 1995; Martinez et al., 2002] as we confirmed by electron microscopy (Fig. 1). The enrichment of plasma membrane for this isolation method, based on ^{125}I-concanavalin labeling, was previously reported as 12- to 14-fold of increase respect to the homogenate [Benaim et al., 1991].

Our results indicate the presence of, at least, two different potassium conductive pathways in *T. cruzi* plasma membrane enriched fractions. Based on the shift in the reversal potential in 17.5% of the seals a potassium selective channel of intermediate conductance (106 ± 4.3 pS) was recorded. The current–voltage relationship was linear and the open probability was higher at positive potentials (Fig. 2).

The relative permeability ratio P_K/P_{Cl} calculated was about 5, similar to the reported values for potassium channels in *Fasciola hepatica* [Jang et al., 2004] and *Dictyostelium discoideum* [Yoshida et al., 1997]. Further work is necessary to obtain a complete biophysical characterization of this channel as well as its possible cellular functions and molecular identity.

The other potassium conductive pathway was observed in 82.5% of the seals, the activity recorded corresponded to a non-selective cationic channel that we called (TcNSCC). This cationic channel often associated in clusters. Its permeability sequence to monovalent cations corresponds to Eisenman sequence II, indicating a weak electrical field at the pore of the channel [Eisenman and Horn, 1983]. Although the relative permeability ratio of Na^+/K^+ is around 0.7, analyzing the total current on the seal under asymmetrical conditions for both ions, the reduction in the current is similar at all

applied voltages (data not shown). This can be explained as a consequence of the decrease in the unitary conductance for K^+ in the presence of Na^+ or due to a lower number of open channels in the seal. Even if both cations have almost the same permeability, not necessarily the conductance for both is the same, considering that ions with higher binding affinity to amino acids at the selectivity filter can show a lower effective conductance. The other possible explanation for a decrease in the K^+ current in the presence of Na^+ is an anomalous mole fraction effect. According to this theory, channels recorded in solutions with two permeant ions, often conduct less current than in the presence of pure solutions of either, indicating that several ions can interact in the permeation pathway [Eisenman et al., 1986; Nonner et al., 1998]. This effect has been previously reported in non-selective cationic channels from different cell types [Wang and Veenstra, 1997; Wells and Tanaka, 1997; Bae et al., 1999].

These permeability properties of TcNSCC can play an important physiological role for *T. cruzi* considering that at the rectum and in the feces of the insect vector, the concentration of monovalent ions changes from 46 mM to 111 mM for Na^+ and from 41 mM to 358 mM for K^+, depending on the feeding cycles of the insect [Kollien et al., 2001]. Under these extremely variable conditions, TcNSCC can constitute a pathway for influx or efflux of both ionic species.

Unlike other non-selective cation channels [Barros et al., 2001; Prakriya and Lewis, 2002; Staruschenko and Vedernikova, 2002; Owsianik et al., 2006], the permeability of TcNSCC to divalent physiological cations was low. Moreover, Ca^{+2} and Mg^{+2} blocked the channel but with different affinity. In the presence of 10 μM Ca^{+2} a significant reduction in the total current of the seal was observed. This effect was dependent on the ion concentration, with a calculated Ki of about 0.5 mM calcium. Single-channel transitions were difficult to record, but a strong increase in the flickering is suggestive of a higher rate of opening and closing events in the presence of Ca^{+2}. It has been reported that Ca^{+2} can exert a dual effect, activating cation channels at micromolar concentrations and blocking them at a millimolar range. In some other cases, Ca^{+2} can primarily be a blocker of non-selective cation channels at very low concentrations [Staruschenko and Vedernikova, 2002; Estacion et al., 2006; Owsianik et al., 2006].

In the presence of 20 mM Mg^{+2} a decrease in the unitary current of TcNSCC (from 4.78 to 1.79 pA at −80 mV) and also a reduction in the total current of the seal was observed at different voltages. These effects can be explained by a decrease in the unitary conductance, the open probability, or both. This effect has been reported in several non-selective cation channels from vertebrates and plants [Davenport and Tester, 2000; Demidchik and Tester,2002; Llanos et al., 2002; Simon et al., 2004]. More data are necessary to elucidate the mechanism of blockage exerted by Mg^{+2} on TcNSCC. Blockage of K^+ currents by Ca^{+2} and Mg^{+2} has been demonstrated recently in murine endothelial cells [Ledoux et al., 2008] and in oocytes overexpressing small conductance calcium activated potassium channels from rat [Soh and Park, 2001].

The molecular identity of *T. cruzi* potassium conductive pathways is still unknown, but genomic information indicates the presence of at least two different types of potassium channels: a voltage-dependent and a calcium-activated potassium channel (http://tcruzidb.org/tcruzidb). Our efforts are now focused on the cloning, expression and characterization of these molecules, in order to establish whether they correspond to the electrophysiological activities reported in this work or they constitute alternative pathways to monovalent ion permeation.

ACKNOWLEDGMENTS

This work was partially supported by American Heart Association postdoctoral fellowship. We thank Dr. Douglas Pace for helpful discussion and corrections of the manuscript.

REFERENCES

Almanza A, Mercado F, Vega R, Soto E. 2008. Extracellular pH modulates the voltage-dependent Ca2+ current and low threshold K+ current in hair cells. Neurochem Res 33:1435–1441.

Bae YM, Park MK, Lee SH, Ho WK, Earm YE. 1999. Contribution of Ca2+-activated K+ channels and non-selective cation channels to membrane potential of pulmonary arterial smooth muscle cells of the rabbit. J Physiol 514(Pt 3):747–758.

Bai JP, Shi YL. 2001. A patch-clamp study on human sperm Cl− channel reassembled into giant liposome. Asian J Androl 3:185–191.

Barrera FN, Renart ML, Molina ML, Poveda JA, Encinar JA, Fernandez AM, Neira JL, Gonzalez-Ros JM. 2005. Unfolding and refolding in vitro of a tetrameric, alpha-helical membrane protein: The prokaryotic potassium channel KcsA. Biochemistry 44:14344–14352.

Barros LF, Stutzin A, Calixto A, Catalan M, Castro J, Hetz C, Hermosilla T. 2001. Nonselective cation channels as effectors of free radical-induced rat liver cell necrosis. Hepatology 33:114–122.

Benaim G, Losada S, Gadelha FR, Docampo R. 1991. A calmodulin-activated (Ca(2+)-Mg2+)-ATPase is involved in Ca2+ transport by plasma membrane vesicles from *Trypanosoma cruzi*. Biochem J 280:715–720.

Benaim G, Moreno SN, Hutchinson G, Cervino V, Hermoso T, Romero PJ, Ruiz F, de SW, Docampo R. 1995. Characterization of the plasma-membrane calcium pump from *Trypanosoma cruzi*. Biochem J 306(Pt 1): 299–303.

Bernucci L, Henriquez M, Diaz P, Riquelme G. 2006. Diverse calcium channel types are present in the human placental syncytiotrophoblast basal membrane. Placenta 27:1082–1095.

Berrier C, Coulombe A, Houssin C, Ghazi A. 1989. A patch-clamp study of ion channels of inner and outer membranes and of contact zones of *E. coli*, fused into giant liposomes. Pressure-activated channels are localized in the inner membrane. FEBS Lett 259:27–32.

Davenport RJ, Tester M. 2000. A weakly voltage-dependent, nonselective cation channel mediates toxic sodium influx in wheat. Plant Physiol 122: 823–834.

Demidchik V, Tester M. 2002. Sodium fluxes through nonselective cation channels in the plasma membrane of protoplasts from Arabidopsis roots. Plant Physiol 128:379–387.

Derst C, Karschin A. 1998. Evolutionary link between prokaryotic and eukaryotic K+ channels. J Exp Biol 201:2791–2799.

Diamond LS. 1968. Improved method for the monoxenic cultivation of Entamoeba histolytica Schaudinn, 1903 and E. histolytica-like amebae with trypanosomatids. J Parasitol 54:715–719.

Eisenman G, Horn R. 1983. Ionic selectivity revisited: The role of kinetic and equilibrium processes in ion permeation through channels. J Membr Biol 76:197–225.

Eisenman G, Latorre R, Miller C. 1986. Multi-ion conduction and selectivity in the high-conductance Ca++-activated K+ channel from skeletal muscle. Biophys J 50:1025–1034.

Ellekvist P, Colding H. 2006. Transport proteins as drug targets in *Plasmodium falciparum*. New perspectives in the treatment of malaria. Ugeskr Laeger 168:1314–1317.

Ellekvist P, Ricke CH, Litman T, Salanti A, Colding H, Zeuthen T, Klaerke DA. 2004. Molecular cloning of a K(+) channel from the malaria parasite *Plasmodium falciparum*. Biochem Biophys Res Commun 318: 477–484.

Ellekvist P, Maciel J, Mlambo G, Ricke CH, Colding H, Klaerke DA, Kumar N. 2008. Critical role of a K+ channel in Plasmodium berghei transmission revealed by targeted gene disruption. Proc Natl Acad Sci USA 105:6398–6402.

Estacion M, Sinkins WG, Jones SW, Applegate MA, Schilling WP. 2006. Human TRPC6 expressed in HEK 293 cells forms non-selective cation channels with limited Ca2+ permeability. J Physiol 572:359–377.

Gull K. 1999. The cytoskeleton of trypanosomatid parasites. Annu Rev Microbiol 53:629–655.

Hamill OP, Marty A, Neher E, Sakmann B, Sigworth FJ. 1981. Improved patch-clamp techniques for high-resolution current recording from cells and cell-free membrane patches. Pflugers Arch 391:85–100.

Henriquez M, Riquelme G. 2003. 17beta-estradiol and tamoxifen regulate a maxi-chloride channel from human placenta. J Membr Biol 191:59–68.

Hille B. 2001. Ion channels in excitable membranes. 3rd. edition, Sinauer, chapter 2, 25–60.

Hosokawa Y, Sandri G, Panfili E, Cherubini E. 1994. Characterization of a voltage-dependent anionic channel in fused synaptosomes isolated from rat hippocampi. Neurosci Lett 169:167–170.

Hughes BA, Swaminathan A. 2008. Modulation of the Kir7.1 potassium channel by extracellular and intracellular pH. Am J Physiol Cell Physiol 294: C423–C431.

Jang JH, Kim SD, Park JB, Hong SJ, Ryu PD. 2004. Ion channels of Fasciola hepatica incorporated into planar lipid bilayers. Parasitology 128:83–89.

Kemp PJ, Peers C. 2007. Oxygen sensing by ion channels. Essays Biochem 43:77–90.

Kollien AH, Grospietsch T, Kleffmann T, Zerbst-Boroffka I, Schaub GA. 2001. Ionic composition of the rectal contents and excreta of the reduviid bug Triatoma infestans. J Insect Physiol 47:739–747.

Lahiri S, Roy A, Baby SM, Hoshi T, Semenza GL, Prabhakar NR. 2006. Oxygen sensing in the body. Prog Biophys Mol Biol 91:249–286.

Lang F, Foller M, Lang KS, Lang PA, Ritter M, Gulbins E, Vereninov A, Huber SM. 2005. Ion channels in cell proliferation and apoptotic cell death. J Membr Biol 205:147–157.

Ledoux J, Bonev AD, Nelson MT. 2008. Ca2+-activated K+ channels in murine endothelial cells: Block by intracellular calcium and magnesium. J Gen Physiol 131:125–135.

Llanos P, Henriquez M, Riquelme G. 2002. A low conductance, non-selective cation channel from human placenta. Placenta 23:184–191.

Long SB, Campbell EB, MacKinnon R. 2005. Crystal structure of a mammalian voltage-dependent Shaker family K+ channel. Science 309: 897–903.

Long SB, Tao X, Campbell EB, MacKinnon R. 2007. Atomic structure of a voltage-dependent K+ channel in a lipid membrane-like environment. Nature 450:376–382.

MacKinnon R, Cohen SL, Kuo A, Lee A, Chait BT. 1998. Structural conservation in prokaryotic and eukaryotic potassium channels. Science 280:106–109.

Martinez R, Wang Y, Benaim G, Benchimol M, de SW, Scott DA, Docampo R. 2002. A proton pumping pyrophosphatase in the Golgi apparatus and plasma membrane vesicles of *Trypanosoma cruzi*. Mol Biochem Parasitol 120:205–213.

Morais Cabral JH, Lee A, Cohen SL, Chait BT, Li M, MacKinnon R. 1998. Crystal structure and functional analysis of the HERG potassium channel N terminus: A eukaryotic PAS domain. Cell 95:649–655.

Nagakura K, Tachibana H, Kaneda Y, Sekine T. 1986. Subcellular fractionation of *Trypanosoma cruzi*; isolation and characterization of plasma membranes from epimastigotes. Tokai J Exp Clin Med 11:23–29.

Nolan DP, Voorheis HP. 2000. Factors that determine the plasma-membrane potential in bloodstream forms of *Trypanosoma brucei*. Eur J Biochem 267: 4615–4623.

Nonner W, Chen DP, Eisenberg B. 1998. Anomalous mole fraction effect, electrostatics, and binding in ionic channels. Biophys J 74:2327–2334.

Owsianik G, Talavera K, Voets T, Nilius B. 2006. Permeation and selectivity of TRP channels. Annu Rev Physiol 68:685–717.

Park JK, Kim YC, Sim JH, Choi MY, Choi W, Hwang KK, Cho MC, Kim KW, Lim SW, Lee SJ. 2007. Regulation of membrane excitability by intracellular pH (pHi) changers through Ca2+-activated K+ current (BK channel) in single smooth muscle cells from rabbit basilar artery. Pflugers Arch 454:307–319.

Ponte-Sucre A, Campos Y, Fernandez M, Moll H, Mendoza-Leon A. 1998. Leishmania sp.: Growth and survival are impaired by ion channel blockers. Exp Parasitol 88:11–19.

Ponte-Sucre A, Mendoza-Leon A, Moll H. 2001. Experimental leishmaniasis: Synergistic effect of ion channel blockers and interferon-gamma on the clearance of Leishmania major by macrophages. Parasitol Res 87:27–31.

Prakriya M, Lewis RS. 2002. Separation and characterization of currents through store-operated CRAC channels and Mg2+-inhibited cation (MIC) channels. J Gen Physiol 119:487–507.

Riquelme G, Lopez E, Garcia-Segura LM, Ferragut JA, Gonzalez-Ros JM. 1990. Giant liposomes: A model system in which to obtain patch-clamp recordings of ionic channels. Biochemistry 29:11215–11222.

Rohloff P, Docampo R. 2008. A contractile vacuole complex is involved in osmoregulation in *Trypanosoma cruzi*. Exp Parasitol 118:17–24.

Rohloff P, Rodrigues CO, Docampo R. 2003. Regulatory volume decrease in *Trypanosoma cruzi* involves amino acid efflux and changes in intracellular calcium. Mol Biochem Parasitol 126:219–230.

Sabirov RZ, Dutta AK, Okada Y. 2001. Volume-dependent ATP-conductive large-conductance anion channel as a pathway for swelling-induced ATP release. J Gen Physiol 118:251–266.

Simon F, Varela D, Eguiguren AL, Diaz LF, Sala F, Stutzin A. 2004. Hydroxyl radical activation of a Ca(2+)-sensitive nonselective cation channel involved in epithelial cell necrosis. Am J Physiol Cell Physiol 287:C963–C970.

Soh H, Park CS. 2001. Inwardly rectifying current–voltage relationship of small-conductance Ca2+-activated K+ channels rendered by intracellular divalent cation blockade. Biophys J 80:2207–2215.

Staruschenko AV, Vedernikova EA. 2002. Mechanosensitive cation channels in human leukaemia cells: Calcium permeation and blocking effect. J Physiol 541:81–90.

Van der HN, Docampo R. 2000. Intracellular pH in mammalian stages of *Trypanosoma cruzi* is K+-dependent and regulated by H+-ATPases. Mol Biochem Parasitol 105:237–251.

Van der HN, Docampo R. 2002. Proton and sodium pumps regulate the plasma membrane potential of different stages of *Trypanosoma cruzi*. Mol Biochem Parasitol 120:127–139.

Vieira L, Cabantchik ZI. 1995. Bicarbonate ions and pH regulation of Leishmania major promastigotes. FEBS Lett 361:123–126.

Waller KL, Kim K, McDonald TV. 2008a. *Plasmodium falciparum*: Growth response to potassium channel blocking compounds. Exp Parasitol 120(3): 280–285.

Waller KL, McBride SM, Kim K, McDonald TV. 2008b. Characterization of two putative potassium channels in *Plasmodium falciparum*. Malar J 7:19.

Wang HZ, Veenstra RD. 1997. Monovalent ion selectivity sequences of the rat connexin43 gap junction channel. J Gen Physiol 109:491–507.

Wells GB, Tanaka JC. 1997. Ion selectivity predictions from a two-site permeation model for the cyclic nucleotide-gated channel of retinal rod cells. Biophys J 72:127–140.

Wyneken U, Marengo JJ, Orrego F. 2004. Electrophysiology and plasticity in isolated postsynaptic densities. Brain Res Brain Res Rev 47:54–70.

Yoshida K, Ide T, Inouye K, Mizuno K, Taguchi T, Kasai M. 1997. A voltage- and K+-dependent K+ channel from a membrane fraction enriched in contractile vacuole of *Dictyostelium discoideum*. Biochim Biophys Acta 1325:178–188.

Zhou M, MacKinnon R. 2004. A mutant KcsA K(+) channel with altered conduction properties and selectivity filter ion distribution. J Mol Biol 338:839–846.